Characterization of Chinese patients with myofibrillar myopathy from a single center: expanding the clinico-genetic spectrum

Yue-Bei Luo
Xiangya Hospital Central South University https://orcid.org/0000-0002-1056-0154
Yuyao Peng
Xiangya Hospital Central South University
Yuling Lu
Guangxi Medical University First Affiliated Hospital
Qiuxiang Li
Xiangya Hospital Central South University
Huiqian Duan
Xiangya Hospital Central South University
Fangfang Bi
Xiangya Hospital Central South University
Huan Yang (yangh69@126.com)
https://orcid.org/0000-0003-1523-0338

Research

Keywords: myofibrillar myopathy, filaminopathy, titinopathy, filaminopathy, BAG3opathy, FHL1opathy

Posted Date: November 28th, 2019

DOI: https://doi.org/10.21203/rs.2.17905/v1

Abstract

Background: Myofibrillar myopathy is a group of hereditary neuromuscular disorders characterized by dissolution of myofibrils and abnormal intracellular accumulation of Z disc-related proteins. We aimed to characterize the clinical, physiological, pathohistological and genetic features of Chinese myofibrillar myopathy patients from a single neuromuscular center.

Methods: a total of 18 patients were enrolled. Demographic and clinical data were collected. Laboratory investigations, electromyography and cardiac evaluation was performed. Routine and immunohistochemistry stainings against desmin, αB-crystallin and BAG3 of muscle specimen were carried out. Finally, next-generation sequencing of genes associated with hereditary neuromuscular disorders were performed.

Results: twelve pathogenic variants in DES, BAG3, FLNC, FHL1 and TTN were identified, of which 7 were novel mutations. The novel DES c.1256C>T substitution is a high frequency mutation. The combined recessively/dominantly transmitted c. 19993G>T and c. 107545delG mutations in TTN gene cause a limb girdle muscular dystrophy phenotype with the classical myofibrillar myopathy histological changes.

Conclusions: we report for the first time that hereditary myopathy with early respiratory failure patient can have peripheral nerve and severe spine involvement. The mutation in Ig-like domain 16 of FLNC is associated with the limb girdle type of filaminopathy, and the mutation in Ig-like domain 18 with distal myopathy type. These findings expand the phenotypic and genotypic correlation spectrum of myofibrillar myopathy.

Introduction

Myofibrillar myopathy (MFM) is a group of hereditary neuromuscular disorders characterized by dissolution of myofibrils and abnormal intracellular accumulation of proteins, which are the constitutive or functional components of the Z disc. The defining morphological features of MFM are streaming, thickening or dissolution of Z disc on electron microscopy. Other characteristic light microscopic changes are eosinophilic materials, rimmed vacuoles and amorphous deposits and rubbed out fibers. Despite the common histological features, significant variation exists in each subtype in terms of clinical manifestation and molecular basis.

There is an ever-expanding panel of genes associated with myofibrillar myopathies including *DES*, *CRYAB*, *MYOT*, *ZASP*, *FLNC*, *BAG3*, *FHL1*, *TTN*, *PYROXD1* and *KY*, which encode proteins that are the integral part of or functionally associated with Z disc. Meanwhile, there are case reports in which other mutated genes cause histological changes compatible with myofibrillar myopathy. These genes include *ACTA1*, *HSPB8*, *PLEC*, *DNAJB6* and *LMNA*. The majority of MFM patients follow an autosomal dominant inheritance pattern, while less frequently, the disease is transmitted by autosomal recessive or X-linked dominant/recessive pattern.

In this study, we present the clinical, histological, immunohistochemical and genetic analysis in 18 Chinese MFM patients diagnosed in our neuromuscular center. Seven novel mutations in *DES*, *FLNC*, *FHL1* and *TTN* have been identified.

Patients And Methods

Patients

Between 2012 and 2019 in the Department of Neurology, Xiangya Hospital, 18 patients were diagnosed of MFMs based on clinical presentations and myopathological findings.

Clinical data

Demographic and clinical data were collected. Laboratory investigations including blood routine, serum creatine levels, electrocardiogram, echocardiography, electromyography were performed.

Histology and histochemistry

Muscle specimens from biceps brachii or quadriceps femoris of 16 patients were snap frozen by isopropene cooled in liquid nitrogen. Sections of 8um thickness were cut using a cryostat (Leica CM1900). Routine stainings were performed as follows: eosin and hematoxylin (HE), modified trichrome Gomori, NADH, SDH, COX/SDH double stain, acid phosphatase, oil red, PAS, ATPase (pH 4.2, 4.6 and 11). Histological changes such as necrotic and regenerating fibers, eosinophilic bodies and amorphous deposits were counted in six random fields under 200x magnification.

Immunohistochemical studies

Ten micrometer thick serial sections were cut for immunohistochemistry studies. Biopsies from subjects, who were ultimately deemed to be free from muscle disease, were used as normal controls. Sections were blocked by 0.3% hydrogen peroxide in methanol and 10% goat serum in PBS for 30 minutes each, then incubated in primary antibodies against desmin (Abcam, 1:400), alpha-B crystalin (Abcam, 1:500) and bcl-2 associated athanogene 3 (BAG3, Abcam, 1:200) overnight at 4°C. After rinsing in PBS, sections were incubated in biotinylated secondary antibodies for 30 minutes. The Vectastain ABC kit (Vector Laboratories, CA) was used for immunodetection. After developed by DAB, the tissues were counterstained by hematoxylin for 10 seconds, then dehydrated through graded ethanol and cleared in xylene, and finally mounted by resin. The numbers of fibers with focal areas of increased reactivity for desmin, alpha-B crystalin and BAG3 were counted in six random fields under 200x magnification.

Genetic studies

Genomic DNA was isolated from peripheral blood (MyGenostics, Beijing). Detected sequence variants, if present in the dbSNP, HapMap, 1000 Genome, ESP6500, ExAC, or in-house Chinese Exome Database (1500 Chinese Han individuals), were all removed. Deleterious SNVs were predicted by SIFT (sift.bii.astar.edu.sg/), Polyphen-2 (genetics.bwh.harvard.edu/pph2/), and MutationTaster (www.mutationtaster.org/) programs. Candidate SNVs were validated by ABI3730 sequencer.

Results

Overview

All patients were screened for MFM genes. Eleven mutations were identified in *DES*, *BAG3*, *FLNC*, *FHL1* and *TTN* (Table 1), of which 7 were not reported previously. The causative gene for patient 18 remained elusive despite extensive screening for the known genes for hereditary neuromuscular disorders.

Table 1 Genetics of the present MFM patient cohort

Patient no.	Gene	Chromosome	Exon	Nucleotide	Protein	Reference
1	*DES*	2	7	c.1256C>T	p.Pro419Leu	None
2	*DES*	2	7	c.1256C>T	p.Pro419Leu	None
3	*DES*	2	7	c.1256C>T	p.Pro419Leu	None
4	*DES*	2	7	c.1256C>T	p.Pro419Leu	None
5	*DES*	2	6	c.1096_1098delACA	p.Asn366del	[1]
6	*DES*	2	6	c.1096_1098delACA	p.Asn366del	[1]
7	*DES*	2	6	c.1096_1098delACA	p.Asn366del	[1]
8	*DES*	2	6	c.1076_1077ins GGCCAGTGG	p.Glu359delins GluAlaSerGly	None
9	*BAG3*	10	3	c.626C>T	p.Pro209Leu	[2]
10	*BAG3*	10	3	c.626C>T	p.Pro209Leu	[2]
11	*FLNC*	7	36	c.6004−3G>A	splicing	None
12	*FLNC*	7	33	c.5468C>T	P.Thr1823Met	None
13	*FHL1*	X	5	c.386G>A	p.Cys129Tyr	None
14	*TTN*	2	344	c.95134T>C	p.Cys31712Arg	[3-9]
15	*TTN*	2	344	c.95185T>C	p.Trp31729Arg	[10]
16	*TTN*	2	69	c. 19993G>T	p.Glu6665X	None
			363	c. 107545delG	p.Arg35849Glnfs*16	None
17	*TTN*	2	69	c. 19993G>T	p.Glu6665X	None
			363	c. 107545delG	p.Arg35849Glnfs*16	None
18	None	None	None	None	None	None

The clinical features were summarized in Table 2. There was a male predominance with a male to female ratio of 1.6:1. The age of disease onset ranged from 1 to 48 years (mean±SD 25.0±16.3 years) with duration from 1 to 27 years (10.6±8.1 years).

Patient no.	Gender	Age (yr)	Duration (yr)	Weakness	Joint contracture	CK (U/L)	EMG	NCS	Cardiac evaluation
1	M	37	5	Lower proximal	-	747	Myo+neuro	Motor axonal	PI/ right heart+LA enlargement
2	M	33	8	Upper+lower proximal+distal	-	935.7	NA	NA	PI/LA enlargement
3	M	33	3	Lower distal	-	1366	Myo	Normal	Frequent APB+ CRBBB+LAFB/ LA enlargement
4	F	45	8	Upper+lower proximal+distal	-	383.4	Myo	Normal	NA
5	M	42	1	Lower distal	-	227.7	Myo	Normal	CRBBB
6	M	30	6	Lower proximal	-	1568.2	Myo	Normal	CRBBB/LA enlargement
7	M	48	19	Upper+lower proximal+distal	-	75.3	Myo	Normal	PI
8	M	13	20	Upper+lower proximal+distal	-	1016.5	Myo	Normal	Normal
9	F	5	20	Lower distal	Achilles tendon/ rigid spine	374.2	Myo+neuro	Motor+ sensory axonal	Obstructive hypertrophic cardiomyopathy
10	F	9	10	Lower proximal+distal scapular winging	Achilles tendon/ talipes cavus/ scoliosis	1269.7	Neuro	Motor+ sensory axonal	Mild mitral+tricuspid+ pulmonary valve regurgitation
11	M	37	10	Upper distal	MCP/PIP/elbow/scoliosis	691.3	Myo+neuro	Normal	NA
12	F	35	6	Lower proximal	-	259.2	Myo+neuro +myotonic	Normal	Normal
13	F	6	2	Lower proximal+distal	-	450.8	myo+ myotonic	Normal	Mild mitral+tricuspid regurgitation
14	M	42	10	Upper+lower distal	-	302.1	Neuro	Motor+ sensory axonal	LAFB/ LA enlargement
15	M	15	5	Upper+lower proximal+distal	Achilles tendon/ scoliosis	340.5	Myo	Normal	Atrial septal defect closure
16	F	1	27	Lower proximal+distal	Talipes cavus/ scoliosis	375.1	Myo	Normal	Mild mitral+tricuspid+ pulmonary valve regurgitation
17	F	1	26	Lower proximal+distal	Talipes cavus/ scoliosis	296	Myo	Normal	NA
18	M	18	5	Lower proximal	-	993.2	Neuro	Motor axonal	Mild mitral+tricuspid regurgitation

Table 2 Clinical features the MFM patients

CRBBB, complete right bundle branch block; LA, left atrium; LAFB, left anterior fascicular block; NA, not available; neuro, neurogenic; NCS, nerve conduction studies; myo, myogenic; PI, pacemaker implant

Upon the first visit to our department, all patients complained of slowly progressive weakness. Apart from one filaminopathy patient who presented with finger muscle atrophy, all cases demonstrated a more severe involvement of the lower limbs. Half of the patients demonstrated a mixed proximal and distal pattern of weakness, 27.8% had predominantly proximal distal weakness and 22.2% proximal. Of note, all four patients with *TTN* mutations displayed a selective anterior tibialis involvement. Seventy-seven-point-eight percent of patients showed muscle wasting, 33.3% experienced prolonged dyspnea. Dysphagia/dysphonia was present in 16.7% of patients, paresthesia/hypesthesia in 22.2%. Joint abnormalities were found in 35.3% of patients, including joint contracture, scoliosis and rigid spine.

Serum creatine kinase levels were mildly to moderately elevated (700.8±440.3U/L).

Of the 15 patients who underwent heart assessment, 13 exhibited cardiac involvement. Both cardiac structural and electrophysical abnormalities were found in 33.3% of cases, 40.0% had only structural changes, and 13.3% only arrhythmia. The types of arrhythmias included bundle branch block and atrial/ventricular premature beat. Structural heart abnormalities included ventricle thickening, atrium enlargement and valve regurgitation. The atrial septal defect in patient 17 was considered incidental.

Nerve conduction study (NCS) and electromyography (EMG) were performed in 17 patients. Nine patients (52.9%) demonstrated pure myogenic changes including MUAPs with short duration and low amplitude. Of these, one patient with *FLNC* mutation and one with *FHL1* mutation also showed myotonic discharges. Four patients (23.5%) showed mixed myopathic and neuropathic features. On NCS, six patients (35.3%) demonstrated peripheral nerve involvement consistent with an axonal type. Motor nerves were preferentially involved in these patients.

Findings on muscle pathology were summarized in Table 3 and presented in the following sections.

Table 3 Myopathological changes of the MFM patients

Patient no.	Necrosis (%)	Regeneration (%)	Central nuclei (%)	Eosinophilic bodies (%)	Cytoplasmic bodies (%)	Amorphous deposits (%)	Non-rimmed vacuoles (%)	Rimmed vacuoles (%)	Rubbed out fibers (%)	Desmin (%)	BAG3 (%)	αB crys (%)
1	0.9	0.5	15.0	6.6	0.5	16.0	0.2	0.1	5.6	12.8	9.2	14.1
2	NA	NA	NA	NA	NA	NA	NA	NA	NA	NA	NA	NA
3	2.9	2.1	22.2	3.1	2.5	3.8	11.5	3.5	6.5	19.7	3.8	3.3
4	1.1	0.9	9.5	1.5	0.4	4.9	2.5	1.5	6.8	5.5	1.8	1.5
5	0.1	0.4	38.4	6.0	0.6	5.1	0.4	0.0	5.3	9.0	3.6	3.4
6	0.2	0.3	11.1	2.2	1.1	4.1	0.2	0.0	2.3	3.7	3.1	4.6
7	NA	NA	NA	NA	NA	NA	NA	NA	NA	NA	NA	NA
8	0.6	0.0	3.4	0.1	0.0	0.2	0.0	0.0	0.1	1.0	0.1	0.2
9	0.3	0.1	1.0	0.5	6.7	6.8	0.0	0.0	0.8	6.4	5.7	6.5
10	0.4	0.0	1.8	2.4	1.4	2.2	0.4	0.0	2.0	4.3	3.6	2.3
11	0.6	0.4	12.4	0.0	0.0	0.0	0.4	1.8	0.0	0.0	0.0	0.0
12	0.3	0.2	18.5	0.0	0.0	0.0	0.9	0.6	0.0	0.0	0.0	0.0
13	0.1	0.0	10.0	2.4	4.4	1.0	0.0	0.0	0.0	0.2	0.0	0.5
14	1.3	0.9	31.4	1.1	4.5	0.0	0.2	0.0	1.4	5.0	1.8	3.9
15	0.0	0.2	10.5	0.2	0.0	0.0	0.0	0.0	0.4	0.8	0.3	0.0
16	0.5	1.1	86.8	0.1	0.3	0.3	2.6	4.0	0.9	4.3	1.8	0.0
17	1.3	0.6	79.3	0.4	0.6	11.9	2.9	0.3	0.0	8.8	1.5	0.8
18	2.7	0.7	36.7	1.8	0.0	2.0	2.0	0.0	0.7	1.5	1.1	1.3

Desminopathy

There were four pedigrees with *DES* mutations (Fig 1A to D), and the inheritance pattern was consistent with an autosomal dominant mode. The disease tended to present in adulthood (age of onset 35.1±10.9 years). All eight patients demonstrated lower extremity weakness, four also had upper limb weakness. Three patients had heart pacemaker implantation. Patient 3 also had episodic palpitation and syncope. His grandmother on mother's side, mother and aunt all had sudden death of presumable 'heart problems'. His half-uncle on mother's side had similar lower limb weakness in his thirtieth (II:2 of Figure 1B). Regardless of disease duration, none exhibited joint contractures. The seven patients who finished EMG studies all showed myogenic changes, and the one with mixed myogenic and neurogenic changes was shown to have axonal polyneuropathy with motor involvement. Three cases showed significant structural changes of heart (Table 2). Apart from the three patients with heart implantation, another three showed arrhythmia including atrial premature beat, right bundle block and fascicular block. On muscle biopsy, the fibers with eosinophilic bodies ranged from 0.1% to 6.6%, rimmed vacuoles from null to 3.5%, rubbed out fibers from 0.1% to 6.8%.

Next-generation sequencing of patients 1 and 2 (brothers) revealed two candidate mutations, c.772C>T in *BAG3* and c.1256C>T in *DES*. The *BAG3* variant was previously reported in an individual with long QT interval but no muscle symptoms[11]. The *DES* c.1256C>T variant was also identified in patients 3 and his affected half-uncle, as well as in patient 4. It causes replacement of a conserved proline by leucine. This substitution is listed as of uncertain significance by ClinVar database and is predicted to be probably damaging by PolyPhen-2 software. Based on the homogenous phenotype of these patients, it is most likely

that the *DES* c.1256C>T substitution is the causative mutation. It is also worth mentioning that the *BAG3* c.772C>T variant was also found as the only possible pathogenic variant in another patient from our department, who has proximal limb weakness, scoliosis and scapular winging. Muscle morphology was of mild myopathic changes and lack of any characteristic MFM changes (data not shown). We could not definitively negate the pathogenicity of this variant.

BAG3opathy

The two BAG3opathy patients carried the same c.626C>T mutation, as in accordance with most other BAG3opathy cases. They both presented in childhood and had severe lower limb weakness, especially distal muscles (MRC 2-3/5). Ten years into disease progression, patient 9 developed obstructive hypertrophic cardiomyopathy and type II respiratory failure, with echocardiopathy revealing enlargement of both atriums, as well as thickening of posterior wall of left ventricle, anterior wall of right ventricle and interventricular septum. She was on noninvasive ventilator since then. Both patients had axonal sensorimotor polyneuropathy confirmed by NCS. In fact, the nerve involvement was so extensive and severe that both were initially diagnosed of Charcot-Marie-Tooth disease (CMT). Mild joint abnormalities, including contracture of Achilles tendon and scoliosis, were noticed in both patients. Pathological changes of this group were similar to those with desminopathy, including increased eosinophilic bodies (0.5-2.4%), cytoplasmic bodies (1.6-6.7%), amorphous deposits (2.2-6.8%) and rubbed out fibers (0.8-2.0%) and few vacuoles (0-0.4%) (Fig 2A). Another feature of BAG3opathy patients was that these changes were conspicuous in focal areas while in other field the muscle may appear completely normal (Fig 2C-D).

Filaminopathy

The disease presented at mid-thirtieth. Patient 11 first noticed atrophy of both hands with minimal difficulties in fine motor skills. Ten years later, he developed lower extremity weakness. There was atrophy of his first dorsal interosseous muscles and tibialis anterior. He had mild contracture of metacarpophalangeal, proximal interphalangeal joints and elbows, as well as mild scoliosis. Patient 12 complained of progressive bilateral leg weakness. Both patients exhibited mixed myogenic and neurogenic changes on EMG, but no involvement of peripheral nerves was found in NCS. The myopathological changes in the patients were minimal, with mildly increased central nuclei (12.4% and 18.5%) and occasional rimmed or non-rimmed vacuoles (0.4-1.8%). Immunohistochemical staining against the three Z band associated proteins were unremarkable.

The two patients had *de novo FLNC* mutations. In patient 11, the intronic substitution c.6004+3G>A was not found in general population according to the Human Gene Mutation Database, and was conserved among species (Fig 3). It was likely to cause skipping of exon 36. The p.Thr1823Met missense mutation in patient 12 was predicted to be probably damaging by PolyPhen-2 (score 1.0).

Titinopathy

There were four tininopathy patients. The phenotype of patient 14 and 15 accorded with hereditary myopathy with early respiratory failure (HMERF). Patient 14 presented with distal lower extremity weakness in his early fortieth. The weakness gradually progressed to upper limbs within 3 years. Four years after disease onset, he developed nocturnal dyspnea and soon required noninvasive ventilation. Physical examination revealed distal weakness and hypesthesia below elbow and ankle joints. There was remarkable reduction in the motor CMAP amplitude of his bilateral tibial and common femoral nerves, right median nerves, as well as the sensory CMAP amplitude of bilateral sural nerves. Nerve conduction velocity was of normal range. Patient 15 presented with progressive scoliosis (Fig 4) and mild walking difficulty at age 15. Subsequent spinal fusion surgery when he was 16 did not ameliorate his leg weakness. He developed post-exercise dyspnea at age 19. On the first visit to our clinic, he had severe generalized muscle atrophy, scoliosis and contracture of bilateral Achilles' tendons. Pulmonary function test on follow up visit showed severe restrictive ventilatory defect and artery blood gas revealed type II respiratory failure. Noninvasive ventilation was recommended. On muscle biopsy, the characteristic necklace fibers (Fig 2G, 2H) were found in both patients. Two missense mutations in exon 344 of *TTN* (c. 95134T>C, c.95185T>C) were identified.

Patients 16 and 17 were sisters presenting with similar lower limb weakness. They learnt to walk at one and half years of age, and they always ran more slowly than their peers. The weakness was slowly progressive and later involved upper limbs. The patients were still ambulatory at the time of biopsy. On physical examination, they demonstrated a waddling gait, and mixed proximal and distal weakness throughout four limbs. Atrophy of quadriceps femoris, hamstrings and tibialis anterior were noticed. Both had lordosis and talipes cavus. Their mother had similar yet much milder lower limb weakness presenting in her twentieth. She was still capable of sedentary work and ambulatory in her fiftieth. The father did not complain of any muscle symptoms. Of the third generation of this family, the second son of patient 17 (III:4), who was five years old, had frequent falls. Others were asymptomatic. Muscle biopsies of biceps brachii from the two cases revealed pathological changes of different degrees. The main findings of patient 16 were increased central nuclei (10.5%) and selective type 1 atrophy (Fig 2I, 2J). In comparison, patient 17 demonstrated more severe changes including considerably more central nuclei (86.6%), eosinophilic materials (0.1%) and rimmed vacuoles (0.4%, Fig 2K). On NADH staining, neither patient showed the typical rubbed out fibers, but instead had occasional darkly stained bar-like area around and extending from vacuoles (Fig 2L). Overall, the titinopathy group had the highest levels of central nuclei (52.0±37.0%). The sisters harbored compound heterozygous mutations in *TTN* (Fig 1E). The allele carrying p.Glu6665X nonsense mutation was passed down by their mother, whereas the other allele with p.35849A>Qfs*16 mutation came from the father.

Miscellaneous

Patient 13 managed to reached her developmental milestones until early childhood. Her parents noticed her having frequent falls and a waddling gait from age 6 years. Physical examination revealed marked weakness of neck and lower limbs with asymmetrical peroneal involvement. Biopsy of biceps showed central nuclear fibers (10%), eosinophilic bodies (2.4%) and cytoplasmic bodies (4.4%). Fibers with desmin aggregates accounted for only 0.2% of total. An unreported variant (c.386G>A) in *FHL1* gene was identified. This missense mutation caused substitution of cysteine by tyrosine, which was predicted to be probably damage (score 0.999) according to PolyPhen-2.

Patient 18 whose pathogenic mutations remained unidentified presented with lower limb weakness in young adulthood. He subsequently developed mild dysphagia and quadriceps atrophy. Nerve conduction studies revealed motor axonal neuropathy. His echocardiography at age 23 showed mild mitral and tricuspid regurgitation. Increased central nucleated fibers (36.7%), occasional eosinophilic bodies (1.8%) and fibers focally immunoreactive to desmin (1.5%), αB crystallin (1.1%) and BAG3 (1.3%) were found on muscle biopsy.

Discussion

Since the main pathological event in MFM is considered disintegration of the Z disc, we first present a brief summary on its physiological features with emphasis on MFM-related proteins. The Z disc, whose core structure is formed by α-actinin homodimers, defines the boundaries of a sarcomere unit and provides an anchoring point for sarcomeres by cross-linking the neighboring actin thin filaments. The interaction between α-actinin and actin itself does not suffice to maintain proper contractile functions of sarcomeres. Other integral Z disc proteins also play a part in the Z disc-thin filament connection. For example, ZASP and myotilin are associated with α-actinin and actin respectively [12, 13]. The large protein titin binds to α-actinin and myosin on each terminal, thus serves as an elastic anchor for thick filaments to the Z disc. Another binding partner for titin is FHL1, which is associated with the I band part of titin and acts as a part of mechanosensing machinery [14]. Titin also interacts with filamin C to participate in the stabilization of the Z disc [15]. Filamin C in turn associates with actin, which strengthens the Z disc-thin filament connection. Desmin is one of the most important intermediate filament proteins in striated muscles. It links the Z disc and the costamere complex so as to stabilize the Z disc, and also links the nucleus to cytoskeleton network[16]. Not only the innate defects of the Z disc-associated proteins lead to MFM pathology, disturbance of the turnover homoeostasis of these constitutive proteins also has similar pathogenicity. Under both physiological and stress conditions, the small heat shock protein αB crystallin binds to titin to retain appropriate conformation of the latter and prevent it from denaturation [17, 18]. The chaperone activity of αB crystallin also enables it to assist desmin scaffold assembly [19]. BAG3 is a co-chaperone molecule involved in the protein quality control system, and is dedicated to clearance of aberrant protein aggrgates by means of chaperone-assisted selective autophagy (CASA) and macrophagy [20-22]. It has been shown that BAG3 interacts with αB crystallin and prevents mutant αB crystallin aggregation [23]. Another co-chaperone DNAJB6 interacts with CASA complex that includes BAG3, the exact physiological significance of which needs further exploration [24].

In this retrospective study, we describe the clinical, electromyographical, pathological and genetic characteristics of 18 MFM patients at our neuromuscular clinic. Desminopathy and filaminopathy patients tend to present in adulthood. In comparison, BAG3opathy cases have childhood onset, while titinopathy patients demonstrate a wider range of onset age from infancy to adulthood. Joint involvement is more promiment in BAG3opathy and titinopathy cases, yet is not a feature of desminopathy. Our desminopathy patients exhibit the most severe cardiac electrophysiological abnormalities to the extent that 3 out of 8 patients have undergone pacemaker implantation, whilst no cases of other genotypes require such procedure. Regardless of the genotypes, motor or sensorimotor axonopathy seems to be the predominant form of neuropathy in this cohort. BAG3opathy patients demonstrate the most severe peripheral nerve involvement. There are two case reports of patients with the canonical MFM-related BAG3 mutation displaying a CMT plus rigid spine phenotype [25, 26]. Neither patient manifests signs of cardiomyopathy, which is common among BAG3opathy. Moreover, despite the telltale finding of Z disc disarray in ultrastructural evaluation, no protein aggregation on light microscopy was reported in the two previous cases. In comparison, one of our BAG3opathy patients developed hypertrophic cardiomyopathy ten years after disease onset. Both of our BAG3opathy patients show the characteristic eosinophilic and cytoplasmic bodies, as well as Z disc protein aggregates. Therefore, in the scenario of early onset, slowly progressive symmetrical distal weakness, paresthesia and diffuse axonal changes on EMG, diagnosis of CMT should be made with caution as BAG3opathy can present with the same manifestations. Proof of cardiac muscle involvement serves as a warning sign, and if present, muscle biopsy should be considered to seek for protein aggregation typical of BAG3opathy.

In terms of the molecular genetics of our cohort, *DES* is the most common pathogenic gene linked to MFM, accounting for 44.4% of all cases, followed by *TTN* (22.2%). The types of mutation in *DES* include missense, deletion, and deletion/insertion. The novel c.1256C>T missense substitution seems to be a high frequency mutation with three families and one sporadic case.

The inheritance pattern of *TTN* mutations can be autosomal dominant or recessive, or even the combination of both [3, 27, 28]. In a large cohort of congenital titinopathy caused by autosomal recessive *TTN* mutations, axial weakness, early joint contractures and progressive respiratory deficiency are the predominant clinical manifestations [29]. The muscle pathology consists of increased central nuclei and cores/minicores, which is more indicative of congenital myopathy than MFM [29, 30]. The coexistence of one dominantly and one recessively inherited mutations has been reported in several titinopathy cases with infantile to adult onset [28]. The weakness pattern of these semi-dominant/recessive titinopathy cases is proximal and/or distal limb weakness, whilst pathology is myopathic with or without rimmed vacuoles. The dominant mutations are all tibial muscular dystrophy-related and are located in exon 363 (M-band exon 5), while the recessive mutations are all frameshifting. In the case of patients 16 and 17, the sisters exhibit an infantile onset of limb girdle weakness plus the characteristic tibialis weakness without significant respiratory or cardiac insufficiency. Whilst the elder sister demonstrates a full picture of MFM pathology, the younger one only shows changes consistent with centronuclear myopathy, resembling the autosomal recessive titinopathy cases[29]. Considering the remarkably similar phenotype between the two sisters, a different genetic background other than the compound heterozygous *TTN* mutations is unlikely. Again, we propose that different degrees of MFM pathology may coexist in the same patient and sampling bias may be the cause of discrepant morphological findings. The *TTN* gene inheritance of patients 16 and 17 follows a combined autosomal recessive and dominant pattern. The frameshifting c.107545delG mutation is situated in exon 363 and passed down by an autosomal recessive fashion, as carriers of this single variant in the family are all asymptomatic. The dominantly inherited c.19993G>T nonsense mutation results in the creation of a premature stop codon in the tandem immunoglobulin domain of the I-band part of titin. Whether this mutation is partially or completely penetrated needs further follow up of the third generation of this pedigree, as only one out of three offspring (III:4 of Fig 1E) that carry the nonsense mutation is manifesting.

So far, the mutations associated with the HMERF phenotype are all located in exon 344 of *TTN*, which is in the 119th fibronectin 3 region of the A-band part of titin. The c. 95134T>C missense mutation of patient 14 was first associated with HMERF in three Scandinavian families[3] and later in various ethnic groups including the Chinese population [4-10]. It is noteworthy that over 100 reported cases of HMERF, peripheral nerves were considered spared [31]. Our patient is the first HMERF patient that shows peripheral nerve involvement, which is consistent with an axonal sensorimotor polyneuropathy pattern. The recurrent c.95185T>C mutation patient 15 carries was reported in one German HMERF family presenting with both proximal and distal weakness [10]. Contracture of Achilles tendon and rigid spine has been reported in some HMERF cases, severe joint abnormalities are nevertheless not the predominant feature of HMERF. The early and severe involvement of spine in patient 15 is reminiscent of an Emery-Dreifuss muscular dystrophy phenotype, which has been reported in recessive titinopathy cases[32]. Taken together, the titinopathy patients in the present study illustrate that: 1. the inheritance pattern of *TTN* is dependent on the malignant level of the mutation, which is at least partially determined by factors such as location, type, as well as the underlying pathomechanisms connected to the mutation; 2. titinopathy is a spectrum of disease entity with a plethora of combination of involved systems, disease manifestation and temporal progression, and pathologies.

At least three phenotypes have been associated with filaminopathy. The first is an adult onset with predominant distal upper limb weakness with non-specific myopathic changes on muscle biopsy and lack of conspicuous intramuscular protein aggregation[33-35]. Mutations in the N-terminal and Ig-like domain 15 of *FLNC* are related to this collective group. The second phenotype is characterized by adult onset of limb girdle weakness and the typical MFM pathology. So far mutations in Ig-like domains 7, 22 and 24 have been linked to this phenotype[36-38]. Recently, a third group of filamiopathy, which is clinically delineated by restrictive cardiomyopathy and congenital myopathy, has been reported[39]. The causative mutations are in Ig-like domain 10. We report that the intronic variant possibly disrupting proper splicing of the region coding for Ig-like domain 18 is associated with the distal myopathy phenotype, and the novel c.5468C>T missense mutation in Ig-like domain 16 can cause the limb girdle phenotype.

Conclusions

To conclude, in the present Chinese MFM cohort, desminopathy is the most common MFM subtype. The novel *DES* c.1256C>T substitution is a high frequency mutation. Sensorimotor axonopathy is the most common form of peripheral neuropathy in MFM patients. BAG3opathy has the most severe peripheral nerve involvement that can mimic CMT both clinically and electromyographically. We also find that combined recessive/dominant *TTN* mutations can cause a limb girdle muscular dystrophy phenotype with the characteristic MFM pathology. Patients with HMERF can have peripheral nerve, as well as severe spine involvement. The mutation in Ig-like domain 16 is associated with the limb girdle type of filaminopathy, and the mutation in Ig-like domain 18 with distal myopathy type.

To conclude, in the present Chinese MFM cohort, desminopathy is the most common MFM subtype. The novel *DES* c.1256C>T substitution is a high frequency mutation. Sensorimotor axonopathy is the most common form of peripheral neuropathy in MFM patients. BAG3opathy has the most severe peripheral nerve involvement that can mimic CMT both clinically and electromyographically. We also find that combined recessive/dominant *TTN* mutations can cause a limb girdle muscular dystrophy phenotype with the characteristic MFM pathology. Patients with HMERF can have peripheral nerve, as well as severe spine involvement. The mutation in Ig-like domain 16 is associated with the limb girdle type of filaminopathy, and the mutation in Ig-like domain 18 with distal myopathy type.

Declarations

Acknowledgements

None.

Authors' contributions

YBL and HY designed this study. YBL wrote and HY revised this manuscript. YL and YP collected the data. FB, QL and QD contributed to the muscle pathological evaluation.

Funding

This work was supported by National Natural Science Foundation of China (grant number 81601094).

Availability of data and materials

The datasets used and/or analysed during the current study are available from the corresponding author on reasonable request.

Ethics approval and consent to participate

Written consent forms were signed by all patients. This study was approved by the Ethics Committee of Xiangya Hospital (reference number 201603284).

Consent for publication

All participants gave approval for publication of anonymized personal data.

Competing interests

None.

References

1. Kaminska A, Strelkov SV, Goudeau B, et al. Small deletions disturb desmin architecture leading to breakdown of muscle cells and development of skeletal or cardioskeletal myopathy. Hum Genet 2004;114(3):306-13.
2. Selcen D, Muntoni F, Burton BK, et al. Mutation in BAG3 causes severe dominant childhood muscular dystrophy. Ann Neurol 2009;65(1):83-9.
3. Ohlsson M, Hedberg C, Bradvik B, et al. Hereditary myopathy with early respiratory failure associated with a mutation in A-band titin. Brain 2012;135(Pt 6):1682-94.
4. Pfeffer G, Elliott HR, Griffin H, et al. Titin mutation segregates with hereditary myopathy with early respiratory failure. Brain 2012;135(Pt 6):1695-713.
5. Uruha A, Hayashi YK, Oya Y, et al. Necklace cytoplasmic bodies in hereditary myopathy with early respiratory failure. J Neurol Neurosurg Psychiatry 2015;86(5):483-9.
6. Yue D, Gao M, Zhu W, et al. New disease allele and de novo mutation indicate mutational vulnerability of titin exon 343 in hereditary myopathy with early respiratory failure. Neuromuscul Disord 2015;25(2):172-6.
7. Pfeffer G, Barresi R, Wilson IJ, et al. Titin founder mutation is a common cause of myofibrillar myopathy with early respiratory failure. J Neurol Neurosurg Psychiatry 2014;85(3):331-8.
8. Palmio J, Leonard-Louis S, Sacconi S, et al. Expanding the importance of HMERF titinopathy: new mutations and clinical aspects. J Neurol 2019;266(3):680-90.
9. Toro C, Olive M, Dalakas MC, et al. Exome sequencing identifies titin mutations causing hereditary myopathy with early respiratory failure (HMERF) in families of diverse ethnic origins. BMC Neurol 2013;13(29).
10. Palmio J, Evila A, Chapon F, et al. Hereditary myopathy with early respiratory failure: occurrence in various populations. J Neurol Neurosurg Psychiatry 2014;85(3):345-53.
11. Lee HC, Cherk SW, Chan SK, et al. BAG3-related myofibrillar myopathy in a Chinese family. Clin Genet 2012;81(4):394-8.
12. Lin X, Ruiz J, Bajraktari I, et al. Z-disc-associated, alternatively spliced, PDZ motif-containing protein (ZASP) mutations in the actin-binding domain cause disruption of skeletal muscle actin filaments in myofibrillar myopathy. J Biol Chem 2014;289(19):13615-26.
13. Salmikangas P, van der Ven PF, Lalowski M, et al. Myotilin, the limb-girdle muscular dystrophy 1A (LGMD1A) protein, cross-links actin filaments and controls sarcomere assembly. Hum Mol Genet 2003;12(2):189-203.
14. Sheikh F, Raskin A, Chu PH, et al. An FHL1-containing complex within the cardiomyocyte sarcomere mediates hypertrophic biomechanical stress responses in mice. J Clin Invest 2008;118(12):3870-80.
15. Gonzalez-Morales N, Holenka TK, Schock F. Filamin actin-binding and titin-binding fulfill distinct functions in Z-disc cohesion. PLoS Genet 2017;13(7):e1006880.
16. Chapman MA, Zhang J, Banerjee I, et al. Disruption of both nesprin 1 and desmin results in nuclear anchorage defects and fibrosis in skeletal muscle. Hum Mol Genet 2014;23(22):5879-92.
17. Bullard B, Ferguson C, Minajeva A, et al. Association of the chaperone alphaB-crystallin with titin in heart muscle. J Biol Chem 2004;279(9):7917-24.
18. Hu Z, Chen L, Zhang J, et al. Structure, function, property, and role in neurologic diseases and other diseases of the sHsp22. J Neurosci Res 2007;85(10):2071-9.
19. Sharma S, Conover GM, Elliott JL, Der Perng M, Herrmann H, Quinlan RA. alphaB-crystallin is a sensor for assembly intermediates and for the subunit topology of desmin intermediate filaments. Cell Stress Chaperone 2017;22(4):613-26.
20. Gamerdinger M, Kaya AM, Wolfrum U, Clement AM, Behl C. BAG3 mediates chaperone-based aggresome-targeting and selective autophagy of misfolded proteins. EMBO Rep 2011;12(2):149-56.
21. Carra S. The stress-inducible HspB8-Bag3 complex induces the eIF2alpha kinase pathway: implications for protein quality control and viral factory degradation? Autophagy 2009;5(3):428-9.
22. Li F, Xiao H, Hu Z, Zhou F, Yang B. Exploring the multifaceted roles of heat shock protein B8 (HSPB8) in diseases. Eur J Cell Biol 2018;97(3):216-29.
23. Hishiya A, Salman MN, Carra S, Kampinga HH, Takayama S. BAG3 directly interacts with mutated alphaB-crystallin to suppress its aggregation and toxicity. PLoS One 2011;6(3):e16828.

24. Sarparanta J, Jonson PH, Golzio C, et al. Mutations affecting the cytoplasmic functions of the co-chaperone DNAJB6 cause limb-girdle muscular dystrophy. Nat Genet 2012;44(4):450-5, S1-2.
25. Noury JB, Maisonobe T, Richard P, Delague V, Malfatti E, Stojkovic T. Rigid spine syndrome associated with sensory-motor axonal neuropathy resembling Charcot-Marie-Tooth disease is characteristic of Bcl-2-associated athanogene-3 gene mutations even without cardiac involvement. Muscle Nerve 2018;57(2):330-4.
26. Kim SJ, Nam SH, Kanwal S, et al. BAG3 mutation in a patient with atypical phenotypes of myofibrillar myopathy and Charcot-Marie-Tooth disease. Genes Genomics 2018;40(12):1269-77.
27. Zheng W, Chen H, Deng X, et al. Identification of a Novel Mutation in the Titin Gene in a Chinese Family with Limb-Girdle Muscular Dystrophy 2J. Mol Neurobiol 2016;53(8):5097-102.
28. Evila A, Vihola A, Sarparanta J, et al. Atypical phenotypes in titinopathies explained by second titin mutations. Ann Neurol 2014;75(2):230-40.
29. Oates EC, Jones KJ, Donkervoort S, et al. Congenital Titinopathy: Comprehensive characterization and pathogenic insights. Ann Neurol 2018;83(6):1105-24.
30. Ceyhan-Birsoy O, Agrawal PB, Hidalgo C, et al. Recessive truncating titin gene, TTN, mutations presenting as centronuclear myopathy. Neurology 2013;81(14):1205-14.
31. Tasca G, Udd B. Hereditary myopathy with early respiratory failure (HMERF): Still rare, but common enough. Neuromuscul Disord 2018;28(3):268-76.
32. De Cid R, Ben Yaou R, Roudaut C, et al. A new titinopathy: Childhood-juvenile onset Emery-Dreifuss-like phenotype without cardiomyopathy. Neurology 2015;85(24):2126-35.
33. Guergueltcheva V, Peeters K, Baets J, et al. Distal myopathy with upper limb predominance caused by filamin C haploinsufficiency. Neurology 2011;77(24):2105-14.
34. Duff RM, Tay V, Hackman P, et al. Mutations in the N-terminal actin-binding domain of filamin C cause a distal myopathy. Am J Hum Genet 2011;88(6):729-40.
35. Rossi D, Palmio J, Evila A, et al. A novel FLNC frameshift and an OBSCN variant in a family with distal muscular dystrophy. PLoS One 2017;12(10):e0186642.
36. Kley RA, Hellenbroich Y, van der Ven PF, et al. Clinical and morphological phenotype of the filamin myopathy: a study of 31 German patients. Brain 2007;130(Pt 12):3250-64.
37. Tasca G, Odgerel Z, Monforte M, et al. Novel FLNC mutation in a patient with myofibrillar myopathy in combination with late-onset cerebellar ataxia. Muscle Nerve 2012;46(2):275-82.
38. Shatunov A, Olive M, Odgerel Z, et al. In-frame deletion in the seventh immunoglobulin-like repeat of filamin C in a family with myofibrillar myopathy. Eur J Hum Genet 2009;17(5):656-63.
39. Kiselev A, Vaz R, Knyazeva A, et al. De novo mutations in FLNC leading to early-onset restrictive cardiomyopathy and congenital myopathy. Hum Mutat 2018;39(9):1161-72.

Figures

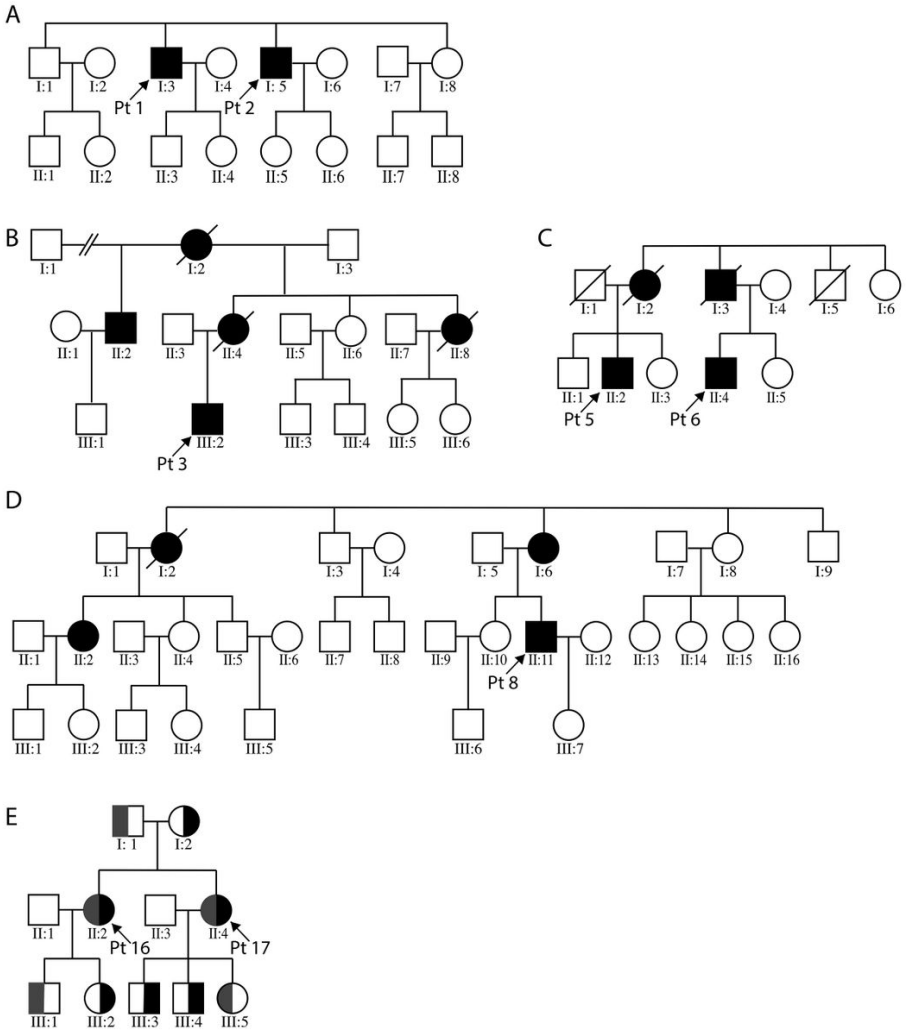

Figure 1

Pedigree charts of the enrolled MFM patients. A-D illustrate the three desminopathy families. E demonstrates the family tree of patients 16 and 17. For 1E, grey bar represents the c. 107545delG mutation carrier, black bar the c. 19993G>T carrier.

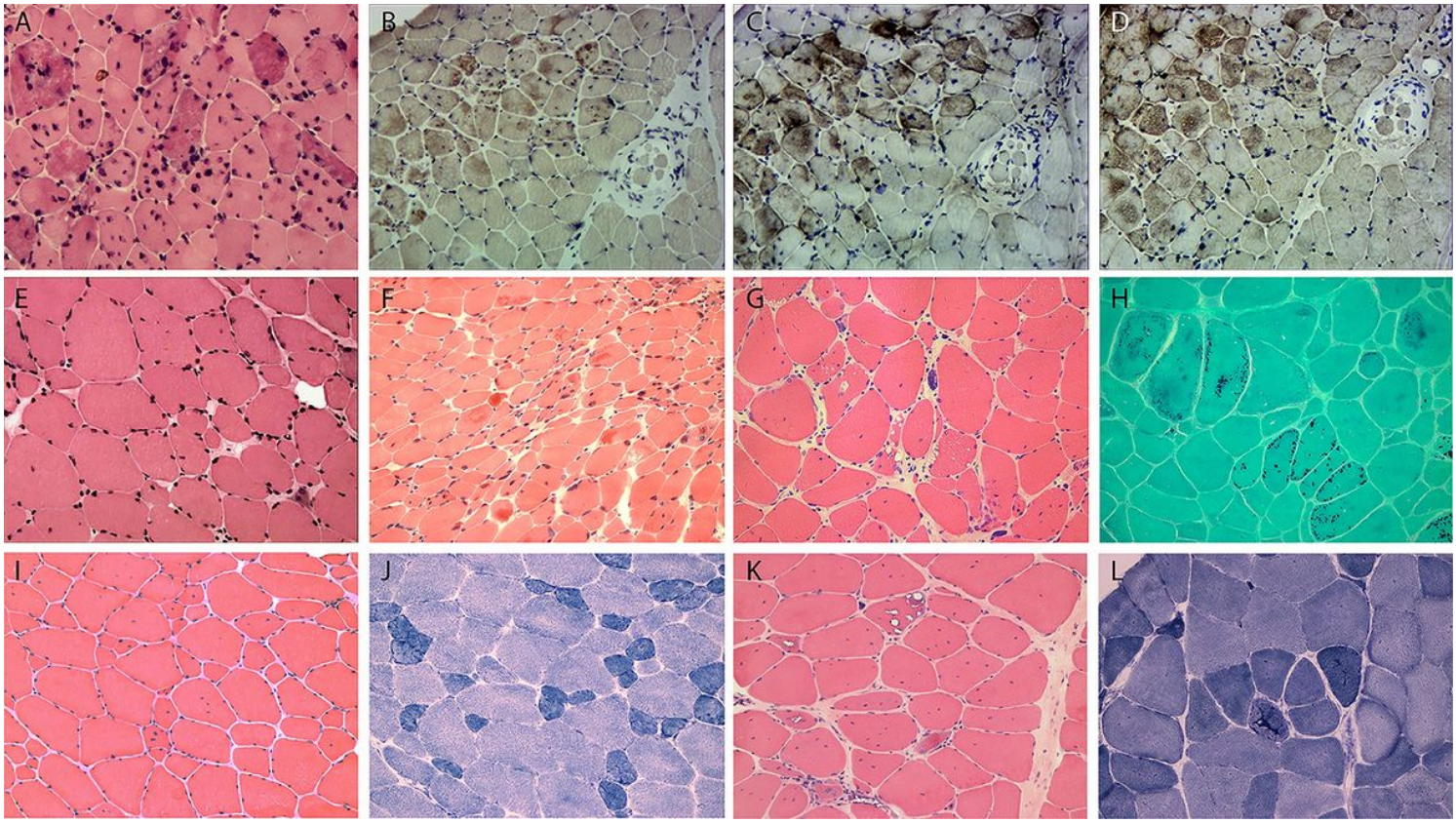

Figure 2

A, HE staining shows the numerous intramuscular eosinophilic deposits in BAG3opathy (patient 9); B-D, immunohistochemistry shows aggregation of MFM-related proteins (B, desmin; C, BAG3; D, αB crystallin). E, HE staining shows fiber size variation and rare regeneration in filaminopathy (patient 11). F, HE demonstrates eosinophilic materials in FHL1opathy (patient 13). Note the overall small fiber size. G, HE shows vacuolated fibers, central nucleated fibers and nuclear clumps in HMERF (patient 15). G, Gomori shows necklace fibers (patient 14). I and J, HE and NADH demonstrates increased central nuclei and selective type 1 atrophy in titinopathy (patient 16). K, HE shows rimmed vacuoles and esosinophilic bodies in titinopathy (patient 17). L, NADH shows relative preservation of the myofibrillar network in the majority of fibers except for occasional rod-like enzyme aggregation in patient 17. Magnification: x200.

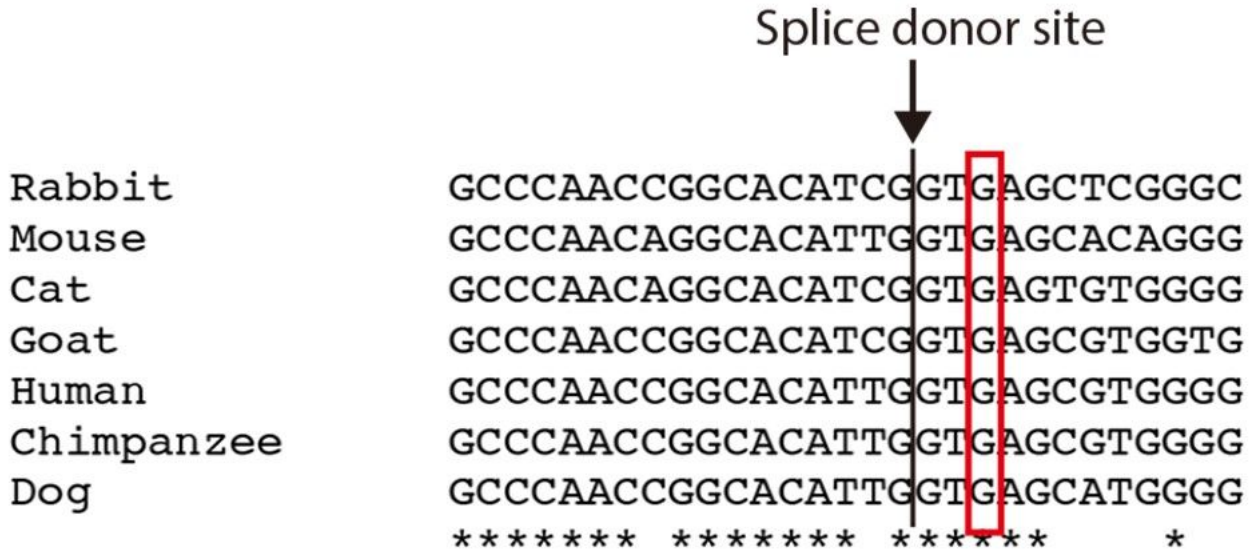

Figure 3

Comparison of the FLNC intronic c.6004+3 nucleotide among different species.

Figure 4

X ray shows severe scoliosis of patient 15 before spine fusion surgery.